JOURNAL OF GUIDANCE, CONTROL, AND DYNAMICS
Vol. 21, No. 2, March–April 1998

Autonomous Navigation of Global Positioning System Satellites Using Cross-Link Measurements

P. A. M. Abusali,* B. D. Tapley,† and B. E. Schutz‡
University of Texas at Austin, Austin, Texas 78712

The Global Positioning System (GPS) Block IIR satellites, which will replace the current Block II/IIA satellites, will have satellite-to-satellite communication capabilities that will allow intersatellite ranging between the Block IIR satellites. The cross-link pseudorange measurements will be used by onboard computers to update the stored navigation messages, which are based on trajectories predicted over an extended period of time, by ground-based processing of tracking data. During normal operations, the cross-link pseudorange measurements will provide improved satellite states, which then can be broadcast to the users. One of the error sources in the updated navigation messages, which cannot be corrected by cross-link measurements, is found in the Earth orientation parameter (EOP) errors. As a consequence, as the age of the Earth rotation parameter increases, the performance of the autonomous navigation system will degrade. The effect of this error source on the Block II GPS autonomous navigation accuracy is described. This work is based on simulated cross-link pseudorange measurements. Realistic force, measurement, and reference frame models are used in the analysis to account for additional major error sources. Cross-link measurements for a period of one day, generated at the end of each of three different prediction intervals, are used to update the predicted trajectory. The estimated solutions then are compared to true solutions to evaluate the effect of prediction errors. With the current EOP prediction errors, the user range errors (URE), computed from improved trajectories and clock differences for a 90-day prediction, exceed 9 m, and for a 180-day prediction, they exceed 17 m. Finally, results of processing measurements from ground stations, instead of cross links, are discussed wherein the URE for the 180-day prediction case are shown to be about 3.1 m.

Introduction

THE current Global Positioning System (GPS), consisting of a 24-satellite cluster, was declared to be fully operational in January 1995. The system has been used over the past decade in a variety of applications in addition to its intended purpose as a navigational aid by the Department of Defense.[1] There has been a phenomenal growth of technology in various fields because of the unprecedented navigation accuracy provided by the GPS data. In applications in which the GPS satellite orbit information contained in the broadcast message is used, the navigation (or the point positioning) accuracy is dependent on the accuracy of the broadcast message.[2] Broadcast message accuracy is controlled by the GPS Operational Control Segment (OCS). A brief description of some of the elements involved in the OCS operations, the context of GPS autonomous navigation, and some of the issues affecting the autonomous operation are described in the following discussion.

The GPS navigation message, broadcast by each satellite, contains information about the orbit of the satellite in the form of Keplerian elements, along with a few additional parameters that approximate the perturbation-related deviation from the two-body ellipse, of the orbit at a given epoch.[3] The navigation applications require that the satellite ephemeris (or the navigation messages) be given in an Earth-centered-Earth-fixed (ECEF) reference frame whose orientation at any time will depend on the Earth rotation. There are 15 parameters broadcast for each satellite at a specified epoch. Using these parameters, a user can compute the position of that GPS satellite in the ECEF reference frame for any time within a certain interval (1 to 2 h) from the epoch time [known as the time of ephemeris (TOE)].[3] The parameters are computed by the OCS for every hour and are uploaded to the satellites, so that the satellites then can broadcast them to the various users.[4] This procedure requires ongoing interaction between the OCS and the Space Segment to provide the orbit information to the satellites. In the event that the ground stations become inoperative, uploading of the orbit information may not be possible for an extended period of time, thereby affecting the usefulness of the GPS as a navigational aid.

As a remedy to such a potential failure, the concept of control system survivability (CSS) was introduced.[5–8] Even if the possibility of an OCS failure is remote, the concept of CSS, when applied routinely, would reduce the level of interaction of the OCS with the Space Segment. This concept is to upload to each satellite predicted orbit information covering a period of 180 days. This information is stored in the onboard computer and used if current OCS uploads are not available. However, because the orbit error will grow proportionally to the prediction interval, orbits predicted over a 180-day period could have large errors and, hence, may not satisfy the accuracy requirements of the system. To improve the accuracy, the CSS concept proposed that the GPS satellites should have the capability to send and receive intersatellite ranging and other information between the satellites in the constellation and should be able to process these measurements onboard to improve the accuracy of the stored orbit information. However, because the ephemeris information is required in an Earth-fixed reference frame, the ability to predict the variations in the Earth rotation is an equally important requirement.

There are several aspects to be considered in applying the cross-link ranging data in the autonomous operation concept. This paper addresses the specific issue of reference frame errors in implementing the concept of cross-link measurements to enhance the stored message accuracy.

Objective

Some of the major steps involved in computing the 15 parameter sets by the OCS are as follows. Tracking data in the form of pseudorange and carrier phase from the GPS satellites are collected continuously from five fixed ground stations distributed around the globe. These stations are shown in Fig. 1. Orbit solutions obtained by processing these data are predicted forward to obtain the ephemeris of each GPS satellite in an ECEF coordinate system. For each satellite, a 4-h (or other appropriate time interval) subset of the ephemeris is processed in a least-squares fitting procedure to obtain a set of 15-parameter navigation messages referenced to the middle of the 4-h duration (TOE).[4] The navigation message for each hour is obtained using a 4-h moving window of the ECEF ephemeris for each

Received June 10, 1996; revision received July 10, 1997; accepted for publication Oct. 26, 1997.

*Research Scientist, Center for Space Research.
†Professor and Director, Center for Space Research. Fellow AIAA.
‡Professor and Associate Director, Center for Space Research. Associate Fellow AIAA.

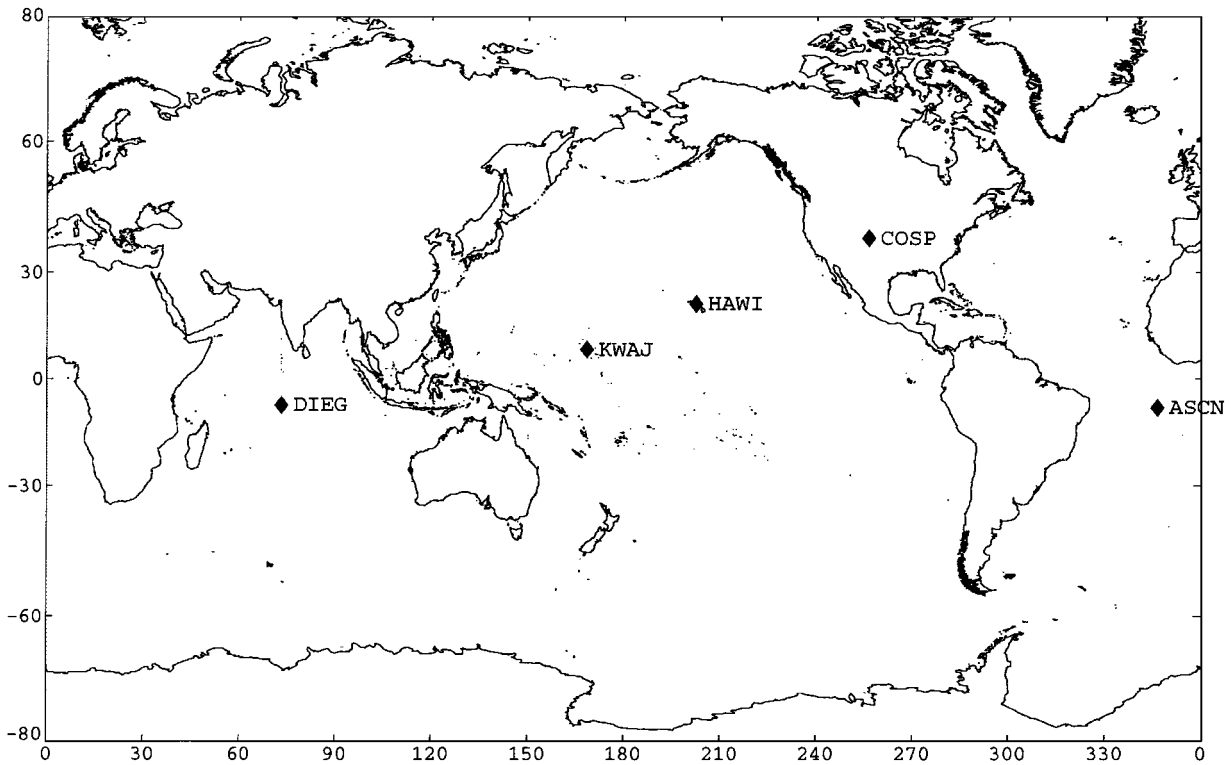

Fig. 1 Ground stations used in the simulation.

satellite. The sequence of 1-h messages is uploaded periodically to the satellites for broadcast to the user community.

In the CSS concept, the orbit determined by the OCS for the navigation message process described is extended by prediction for a period of 180 days past the data-fit time interval, and the 1-h navigation messages are computed as described for the entire 180-day interval. The dynamic model for the GPS satellites, which includes the Earth's gravity field, third-body perturbation models for sun and moon, and the nongravitational forces due to solar radiation pressure (SRP) and thermal effects, is not perfect. Furthermore, the reference frame used in computing the predicted ephemerides will be dependent on predicted values of the Earth orientation parameters (EOPs) that define the orientation of the Earth-fixed reference frame. When cross-link measurements are used onboard the GPS satellite to correct the stored navigation messages, part of the error in the messages due to dynamical model error will be corrected, but the reference-frame error caused by using the predicted values of the EOP (in determining the stored messages) cannot be corrected by the filter-processing cross-link measurements.

The objective of this paper is to assess the level of error present in the stored navigation messages after they are updated, by use of the cross-link measurements. Typical GPS constellation and realistic dynamic error models are assumed in simulating the scenarios and measurements. The variations in the EOP, namely, the polar motion and UT1, are stochastic in nature and therefore are very difficult to predict accurately. An actual realization of EOP prediction error is used.

Assessment Method

In the CSS concept, the cross-link measurements are processed by an onboard computer, using Kalman filter adjustments to the stored navigation messages, which would be the a priori filter states. Suboptimal filters, in which not all of the 15 parameters need to be adjusted, have been proposed. These include adjusting only the six Keplerian elements or just the mean anomaly.[5–8] Results presented in Ref. 8 do not include the effects of Earth orientation error. Further, the orbit errors were simulated using a sinusoidal model with amplitudes chosen for the three position components of the true orbit. This model is deficient in accounting for real orbit errors.

In this paper, the approach taken is to generate true orbits using the best available dynamical-force models and include major systematic error sources to simulate a set of appropriate cross-link measurements. The measurements will have realistic dynamical model and clock error characteristics. Further, the measurements are processed in a least-squares batch mode using a nominal model to estimate the epoch conditions of the satellite state vector. The satellite coordinates are expressed in a rectangular Cartesian inertial coordinate system. The state vector consists of the satellite position and velocity along with one scale parameter for the SRP, one for the Y-bias acceleration, and bias and drift of a linear clock model for each satellite. When ground-station data are processed, the linear-clock-model parameters for ground-station clocks also are included in the estimation state vector. Because the simultaneous estimation of all clock parameters using pseudorange measurements leads to an unobservable case, one of the clocks is considered to be known and is not estimated and, consequently, the estimated values of the other clocks are determined relative to this fixed clock.

Instead of processing the cross-link measurements over the entire period of 180 days, the true and the nominal models are predicted forward using the respective dynamic models. This process allows a realistic realization of the orbit error that occurs in the 180-day prediction. At the end of the prediction period, the cross-link measurements are processed for a short arc length, using the predicted state as the a priori initial condition. The least-squares solution from this fit is compared with the true solution to evaluate the errors present in the cross-link solution for the satellite orbits. This approach is equivalent to adjusting all 15 parameters of the GPS ephemeris broadcast message for the following reason. Values of the 15-parameter broadcast sets for specified epochs (TOEs) are computed by a least-squares fit to the Cartesian components of the predicted trajectories over a period of 4 h. For a typical case, the data fit is usually of the order of a few decimeters, as illustrated in Table 1. (In the tables, SVID is satellite vehicle identification number for simulation.) This indicates that the 15-parameter set of broadcast parameters is equivalent (within a few decimeters) to the trajectory in Cartesian coordinates. Thus, comparing the filtered values of the 15-parameter set to its true values is equivalent to comparing the estimated trajectory to the true trajectory. The least-squares batch processing is performed over a fixed interval of time, and results are generated processing one-day arcs at the end of the prediction period. Three such prediction intervals are considered, namely, 30, 90, and 180 days.

Table 1 Maximum rms of fit of navigation messages[a]

SVID	rms, cm	SVID	rms, cm	SVID	rms, cm
1	42	8	42	15	32
2	60	9	69	16	43
3	70	10	99	17	78
4	56	11	39	18	48
5	69	12	60	19	53
6	47	13	75	20	62
7	75	14	48	21	75

[a] Values were obtained when the 15-parameter navigation messages were fitted to 180 days of predicted trajectory for each satellite, at an interval of 3 min. The fit interval was 4 h for each 15-parameter set. The minimum value of rms of fit was as low as 5 cm for some fit intervals.

The rotation rate of the Earth (corresponding to the UT1) and the orientation of the spin axis (corresponding to the x and y components of the pole position) are unpredictable and result in satellite position errors (in the ECEF) that cannot be neglected for some applications. The nature of variation of polar motion and UT1 is illustrated in Figs. 2a–2c. These can be considered as three different realizations of the random prediction errors of the EOPs. The data used in these plots are from the EOP solutions computed at the Center for Space Research (CSR), University of Texas at Austin, using satellite laser ranging (SLR) data, and such solutions are computed routinely every week (personal communications, R. Eanes, CSR). The figures represent the difference between the true values of (UT1, xp, yp) over the period shown in each figure, which are contained in a current EOP solution, and those that were available at the time of epoch of each figure. For example, for Fig. 2c, the epoch of the plot is April 23, 1995. The EOP solution produced on the week of April 23, 1995, included all SLR data up to that week (quick-look SLR only for a few preceding weeks), and hence the computed solution was very close to the true solution for times preceding this epoch, whereas EOP values past this epoch were predictions. Figure 2c shows the difference for 180 days starting at April 23, 1995, between these predicted values and the corresponding (true) values obtained from one of the most recent EOP solution files (personal communications, R. Eanes, CSR). Figures 2a and 2b were produced in a similar manner.

EOP values corresponding to predictions shown in Fig. 2c are used in the simulation. In other words, the epoch of all prediction arcs (30-, 90-, and 180-day periods) is April 23, 1995, the EOP values computed most recently (for these intervals) are treated as the true values, and those computed during the week of April 23, 1995, are considered to be the nominal values. Thus, for the current simulation, the values shown in Fig. 2c represent the error in the Earth orientation.

Simulation Model

Although the current GPS constellation consists of 24 satellites, in this study a 21-satellite configuration is assumed with six different orbit planes separated by 60 deg in the longitude of the ascending node, each plane being inclined at 55 deg to the Earth's equator. Each plane contains three satellites equally spaced in mean anomaly (MA), and the remaining three satellites are placed in alternative orbit planes at optimal locations. The Keplerian elements for a specified epoch in this configuration are listed for all satellites in Table 2 (Ref. 8). These provide the initial conditions for generating true trajectories and the observations for a specified period of time, using the true force model given in Table 3.

Simulation of the cross-link observations was performed in two stages. In the first stage, the equations of motion in Cartesian coordinates are numerically integrated to obtain true trajectories for all of the satellites. The initial conditions given in Table 2 and the force model in Table 3 (Refs. 9 and 10) were used. Further, clock errors for all of the satellites and the ground stations (26 clocks in all) also were created using the model described later. In the second stage, the true trajectories and the clock errors are input to another program, which computes the distances between satellites and creates cross-link pseudorange measurements by applying the computed clock errors and visibility constraints for the constellation. Visibility is assumed between two cone angles of 32 and 65 deg, with axis of cone being the nadir from GPS satellite transmit antenna.

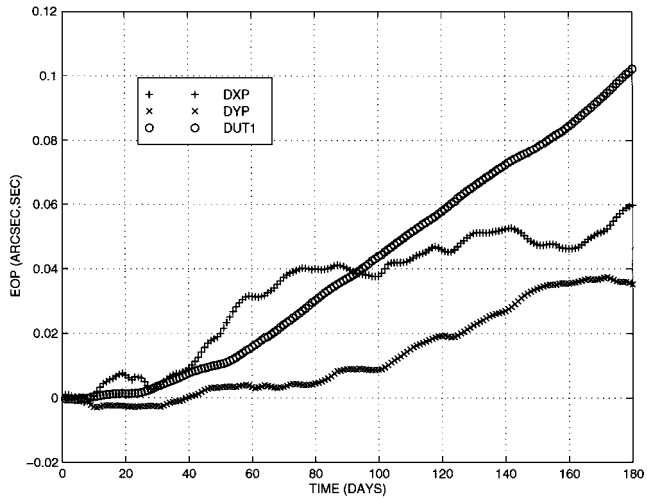

Fig. 2a EOP prediction errors: epoch Feb. 14, 1993.

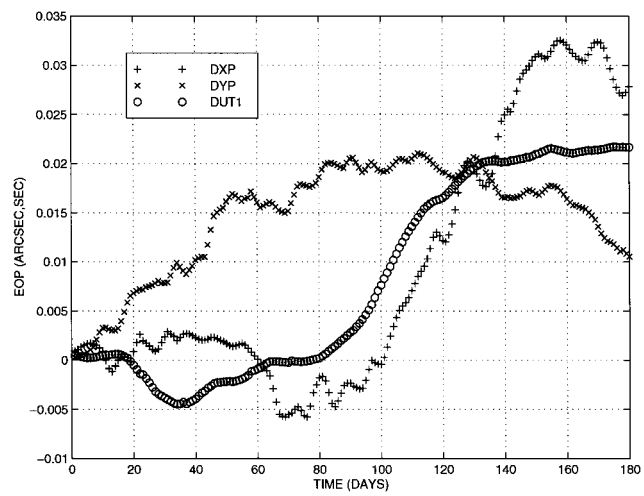

Fig. 2b EOP prediction errors: epoch June 6, 1994.

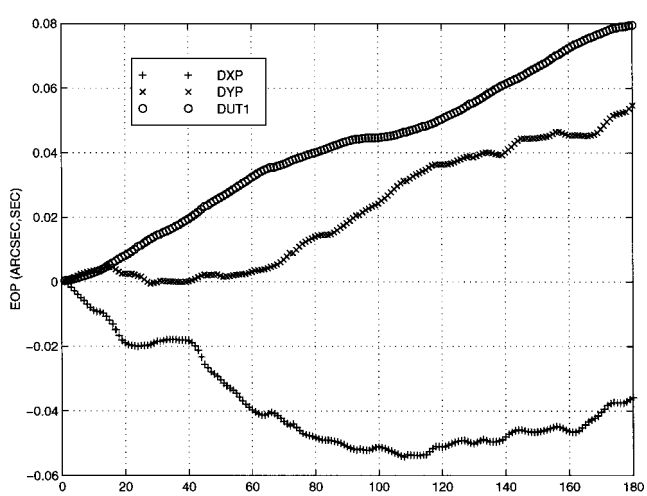

Fig. 2c EOP prediction errors: epoch April 23, 1995.

Measurement errors due to instrument noise (or other random effects) and those due to medium effects (and other systematic effects such as relativity) were not considered in the simulation because the objective was to assess, as clearly as possible, the effect of reference-frame error. For the same reason, the dynamic model, given in Table 3, also was kept as simple as possible, but it does include all major error sources that affect the accuracy of the orbit prediction.

In the cross-link communication mode, each satellite has to transmit information to other satellites and also receive information from

Table 2 Constellation definition assumed for observation simulation[a] (epoch time: April 17, 1995)

SVID	ECC[b]	Node,[c] deg	MA, deg	ETA[d]	ALFA[e]
1	0.001	30.0	137.0	1.010	0.350
2	0.010	30.0	257.0	1.020	0.700
3	0.020	30.0	17.0	1.030	1.050
4	0.005	30.0	167.0	1.020	0.700
5	0.001	90.0	177.0	0.990	−0.350
6	0.010	90.0	297.0	0.980	−0.700
7	0.020	90.0	57.0	0.970	−1.050
8	0.001	150.0	217.0	0.995	−0.500
9	0.010	150.0	337.0	0.985	−0.600
10	0.020	150.0	97.0	0.975	−0.700
11	0.005	150.0	307.0	0.985	−0.600
12	0.010	210.0	257.0	1.000	0.000
13	0.020	210.0	17.0	1.000	0.000
14	0.020	210.0	137.0	1.000	0.000
15	0.001	270.0	297.0	1.005	0.205
16	0.010	270.0	57.0	1.005	0.305
17	0.020	270.0	177.0	1.005	0.405
18	0.005	270.0	87.0	1.005	0.305
19	0.001	330.0	337.0	1.000	0.000
20	0.010	330.0	97.0	1.000	0.000
21	0.020	330.0	217.0	0.990	0.000

[a]Semimajor axis for all satellites, $A = 26559800.0$ m; inclination for all orbit planes, $I = 55$ deg; argument of perigee for satellite, $\omega = 0.0$ deg; mass of each satellite, $M = 814.0$ kg; and effective cross-sectional area, $S = 10\ \text{m}^2$.
[b]Eccentricity.
[c]Longitude of ascending node.
[d]Scale factor for solar radiation pressure acceleration.
[e]Y-bias acceleration scaled by 10^{-9} m/s^2.

Table 3 Force model and reference frame for true trajectory

Force type	Model used in simulation
Earth's gravity	JGM-3 model, truncated to 8×8 (Ref. 9)
Third-body perturbation	(Due to sun and moon only) Jet Propulsion Laboratory Ephemerides, DE200
Solar radiation pressure	ROCK4 Model (Ref. 10)
Thermal effects	Y-bias Model (Ref. 10)
Earth orientation	Current EOP set determined using SLR data

the other satellites. In the current simulation, the assumption is made that, at a given instant of time, only one of the GPS satellites in the constellation can be transmitting and all of the rest of the satellites should be in a receive mode. Consequently, each satellite is allotted a specified time interval during which only it will transmit and the others will receive, and all of the satellites are cycled through such a sequence. The completion of such a sequence is called a burst. In this simulation, the interval for each satellite to transmit is assumed to be 1.5 s, which implies that between 0.0 and 1.5 s of a burst, satellite 1 will transmit and all of the others will receive, satellite 2 will transmit between 1.5 and 3.0 s and all of the others will receive, and so on, until all 21 satellites have gone through a transmit cycle. Thus, the duration for one burst is 31.5 s in this simulation, and for a 24-satellite constellation, the duration will be 36 s. Such bursts of measurements are generated at 15-min intervals for the cross-link and ground-station observation simulation.

To create realistic pseudorange measurements, random clock errors were computed, using the model described next, and added to the computed distances between satellites or between satellites and ground stations. The clock-error characteristics were assumed to be those of a cesium time standard, and appropriate values for the parameters in the clock model were chosen.[11,12] The clock errors are obtained by integration of two first-order differential equations driven by white noise. The differential equations[13] are

$$\frac{\mathrm{d}(\eta_1)}{\mathrm{d}t} = -\omega\eta_1 + (\alpha - 1)\omega u \tag{1}$$

$$\frac{\mathrm{d}(\eta_2)}{\mathrm{d}t} = -\left(\frac{\beta}{\alpha}\right)\eta_1 + \left(\frac{\beta}{\alpha}\right)u \tag{2}$$

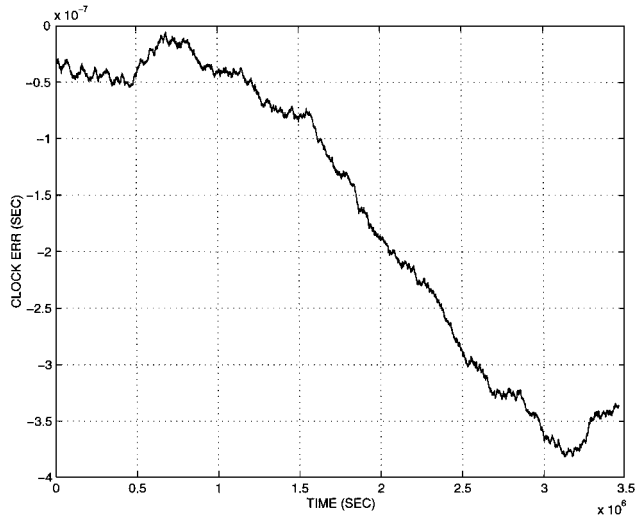

Fig. 3a Simulated SV-1 clock errors for 40 days from April 17, 1995.

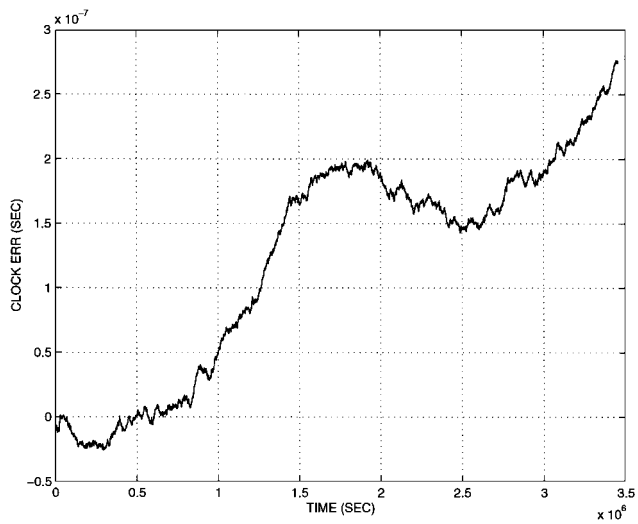

Fig. 3b Simulated GS-1 clock errors for 40 days from April 17, 1995.

where η_2 is the random error of a clock and u is a Gaussian stochastic process with

$$E[u(t)] = 0, \qquad E[u(t_1)\quad u(t_2)] = q \cdot \delta(t_2 - t_1), \qquad q = 1 \tag{3}$$

The values of the parameters used in the current simulation, which are representative of a cesium clock, are as follows:

$$\alpha = 10.0, \qquad \beta = 3.1623 \times 10^{-10}, \qquad \omega = 7.1664 \times 10^{-7}$$

For the present simulation, the initial conditions for the differential equations (1) and (2) were $\eta_1(t_0) = \eta_2(t_0) = 0.0$, where $t_0 =$ April 17, 1995, 00:00:00. The random process $u(t)$ was approximated as a stepwise constant random sequence to find a closed-form solution of the differential equations. The random sequence was started by different seeds to the random-number generator, and this was the identifier for each of the 26 clocks (21 for the GPS satellites and 5 for the ground stations) that were simulated. The differential equations were integrated analytically, and the value of η_2, output at a specified time, represents the random error of the particular clock at that time. For each clock, a table of errors was created at an interval of 450 s. Figures 3a and 3b show the clock errors of GPS SV-1 and of ground-station 1 (Kwajalein), respectively, for the first 40 days from t_0.

Results

To obtain predicted nominal trajectories for the GPS satellites, procedures similar to the actual steps performed by OCS were adopted, so that the prediction errors would be close to the operational prediction errors. Pseudorange measurements from the five ground stations were simulated for a period of six days, from

April 17 to April 23, 1995, based on the true model given in Table 3. These measurements were then processed in a least-squares fit, adjusting all of the satellite states and four ground-station clocks (218 parameters), using a nominal force and reference-frame model. This nominal model differs from the true model in three respects. In the nominal model, 1) the JGM-3 gravity model is replaced by the WGS-84 (truncated to 8 × 8) model[14]; 2) the ROCK4 SRP model is replaced by a simple constant-area model; and 3) the EOP data are from the EOP predicted solution for April 23, 1995. The rms of fit for this solution is about 2.48 m, which includes 15,979 pseudorange measurements from all five stations over six days, generated at 15-min intervals. The solution thus obtained provides the initial conditions for the prediction of the nominal trajectories. This estimated state vector is referred to as $XN(t_0)$ to be used along with the nominal force model to obtain nominal trajectories. The initial conditions corresponding to the elements of Table 2 are referred to as $XT(t_0)$ and are used along with the true force model to produce true trajectories and simulated cross-link measurements.

Results for three different cases are discussed in the following. In each case, cross-link pseudorange measurements are simulated for a period of one day, after the respective prediction period (using the true model), and are processed using the nominal model in a least-squares fit, and the solution then is compared with the true trajectory to compute the user range error (URE) over the one-day fit period. Initial conditions for estimation were obtained by propagating $XN(t_0)$ forward, using the nominal model. The three cases are described in Table 4.

In each of the three cases, cross-link measurements between the 21 satellites only are processed and hence the number of parameters in the estimation state vector is 208. The a priori variances used for adjusted parameters are position components $= 10^{10}$ m^2, velocity components $= 10^2$ (m/s)^2, SRP scale factor $= 10$, Y-bias parameter $= 1$, clock bias $= 10^{18}$ m^2, and clock drift $= 10^2$ (m/s)^2.

Table 5 shows the rms of fit for each satellite in the constellation for case 3.

The prediction errors in the nominal trajectories grow because of the differences between the true and the nominal force models as the prediction interval increases. For case 3, comparing the true trajectory to the predicted trajectory over the one-day period of measurement simulation, namely, over day 187 (counted from t_0), one finds the differences to be of the order of tens of kilometers in the along-track and the cross-track components of the orbits, reaching as large as about 80 km. However, when the cross-link measurements are processed and the solution is compared with the true values, the differences are reduced to about 900 m in the along track (ATRK) and to about 1500 m in the cross track (CTRK). Table 6 shows the mean and rms of these trajectory differences, computed at 15-min intervals over one day.

From the along-track and cross-track rms values of Table 6, it is clear that the cross-link solution has large mean differences when compared with the true solution. However, these differences are not real but are the results of artifacts in the cross-link solution. The information content in the cross-link measurements is such that the longitudinal positioning of the GPS constellation (as each orbit plane precesses because of oblateness of the Earth), with respect to the ECEF frame at any given instant of time, is unobservable. As a result, the estimation solution, when cross-link measurements are processed, contains an arbitrary bias in the estimated values of the longitude of ascending node for each orbit plane. The effect of such a bias is to introduce constant offsets in the horizontal components of the satellite position, as seen in Table 6. Note that these constant offsets group around different values for different planes because the node estimates differ from each other by a small amount. The groupings of the satellites (indicated by the values of the Node in Table 2), are as follows: Satellites 1–4 are in plane A, 5–7 in plane B, 8–11 in plane C, 12–14 in plane D, 15–18 in plane E, and 19–21 in plane F.

Solutions for cases 1 and 2 exhibit similar characteristics. For case 1, the constant offset in the rms values of the along-track components varies between about 20 and 71 m, and that in the rms of cross-track components varies around the 75-m level (comparable to the 1500-m level of Table 6). For case 2, the along-track offset varies around 2200 m and the cross-track component around 4700 m. Unfortunately, the effect of errors in the EOP values on the cross-link solutions, which is the object of this investigation, is completely obscured by these large differences between the estimated and true trajectories.

To further clarify the fact that the large offsets seen in Table 6 are caused by an arbitrary bias introduced in the estimates of the nodes, the estimated constellation and the true constellation are used in a least-squares fit of the seven-parameter Helmert transformation (corresponding to a translation of the origin, rotations about the three axes, and a scale factor).[15] At each trajectory output time point (15 min), a set of seven parameters is estimated and the three Euler angle parameters from these estimates are shown in Fig. 4 for case 2

Table 4 Summary of three simulation experiments

Case no.	No. of days predicted from t_0	Day of measurement simulation counted from t_0	No. of observations processed	rms of fit, m
1	36	Day 37, May 23, 1995	22,294	1.98
2	96	Day 97, July 22, 1995	23,254	1.87
3	186	Day 187, Oct. 22, 1995	23,318	1.87

Table 5 RMS of fit over day 187, for individual satellites (case 3)

SVID	No. of observations processed	rms of fit, m
1	1174	1.88
2	1189	1.81
3	1116	1.86
4	1025	1.81
5	1129	1.90
6	1151	2.05
7	1156	1.83
8	1120	1.72
9	1070	1.90
10	1126	1.83
11	1006	1.80
12	1062	1.99
13	1190	1.81
14	1186	1.93
15	1218	2.09
16	1063	1.93
17	1125	1.81
18	961	1.75
19	1107	1.84
20	1167	1.84
21	977	1.72

Table 6 Summary of one-day trajectory difference between cross-link solution and true values for case 3

Satellite no.	Mean, m			rms, m		
	Radial	ATRK	CTRK	Radial	ATRK	CTRK
1	0.99	552.0	28.5	1.01	666.9	1571.8
2	1.04	563.5	35.2	1.06	678.3	1555.8
3	1.02	558.3	49.0	1.06	672.2	1563.1
4	0.97	551.7	44.9	1.00	666.8	1573.5
5	1.03	531.7	25.2	1.06	649.3	1567.2
6	0.98	531.9	9.9	1.0	650.1	1567.4
7	1.00	537.2	60.8	1.01	657.6	1558.7
8	0.97	668.9	13.1	0.99	763.3	1553.8
9	0.94	658.2	9.5	0.96	754.5	1568.6
10	0.99	665.3	84.9	1.00	760.6	1558.6
11	0.98	660.7	−6.0	0.99	755.7	1565.9
12	1.01	823.4	35.8	1.02	898.5	1537.5
13	0.99	818.9	56.0	1.00	893.2	1543.2
14	0.94	809.5	100.4	0.99	885.9	1557.3
15	0.95	842.3	−19.3	0.97	912.9	1544.3
16	1.00	847.9	28.3	1.03	919.3	1536.7
17	1.02	839.1	98.1	1.03	910.7	1549.2
18	0.99	849.0	24.4	1.02	920.7	1534.3
19	0.98	707.9	−23.0	1.02	796.9	1566.1
20	1.01	717.8	46.4	1.02	805.1	1550.6
21	0.98	715.8	85.7	1.00	803.4	1554.6

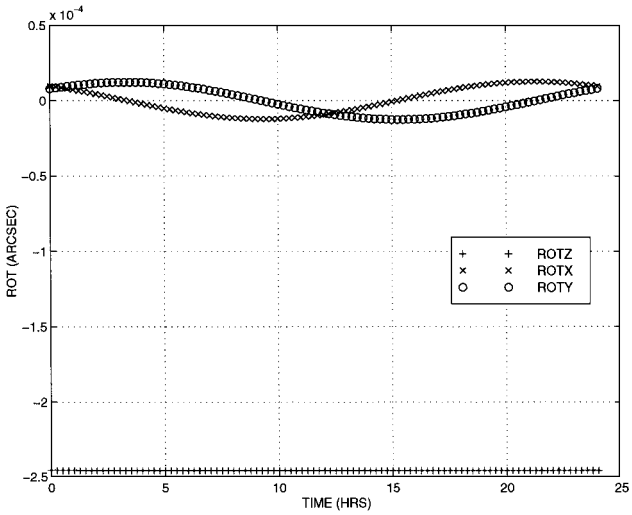

Fig. 4 Euler rotation angles of seven-parameter transformation for case 2.

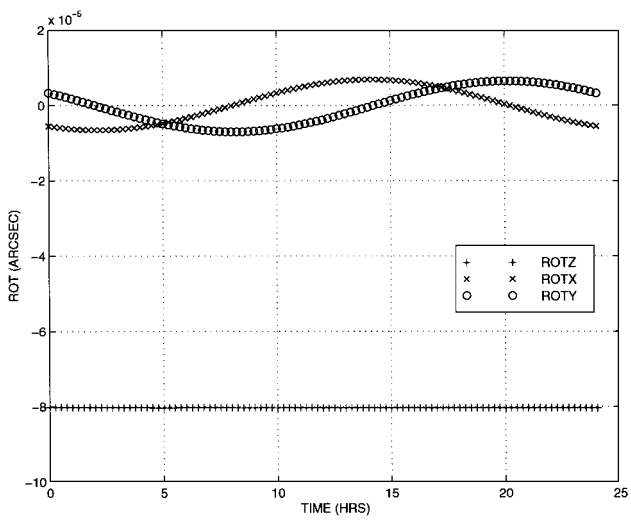

Fig. 5 Euler rotation angles of seven-parameter transformation for case 3.

and in Fig. 5 for case 3. It can be seen clearly that the rotation angle about the Z axis has a large bias.

The bias is caused by numerical unobservability and does not represent the autonomous system performance. Appropriate estimation techniques can remove this arbitrary bias or at least make it negligible, leaving only the deterministic errors that are dominated by the UT1 prediction error. In the autonomous mode, the bias can be isolated and removed after the filter solution, as suggested by Menn and Bernstein.[16] Another approach to handle this bias would be to formulate the filter parameters in terms of Keplerian elements intead of the rectangular Cartesian coordinates and to allow the filter itself to ignore the unobservability of the orbit node, by imposing tight constraints on the covariance of this parameter. The fact that the arbitrary bias mentioned earlier does not affect the system performance is clear by the results of Ref. 6, which shows the rms horizontal position error to be about 35 m after 180 days and by Fig. 7 of Ref. 17, which shows the rms horizontal position error to be under 7.5 m after 180 days. These rms values do not include the effect of UT1 prediction errors but show that the arbitrary bias seen in Table 6 is not real.

The solution trajectory estimated using cross-link measurements is based on the predicted EOP values, but the effects of the prediction errors are not detectable, as mentioned earlier. To determine the EOP prediction-error effect, the cross-link solution is propagated using the true EOP values (used for measurement simulation and true trajectory generation) and the resulting trajectory is compared with the true trajectory. For case 3, these differences, computed over the one-day period, show an rms value of about 56 m for the along-track components (as opposed to the 600- to 900-m level of Table 6) and an rms value of about 112 m for the cross-track components (as opposed to the 1500-m level of Table 6). These differences are used to compute the URE, based on formulas found in Refs. 8 and 18. Figures 6–8 show the URE values computed for the one-day periods in cases 1, 2, and 3, respectively. As can be seen, the prediction error in EOP values results in URE values of more than 9 m for a 90-day prediction stored ephemeris and more than 17-m for a 180-day prediction stored ephemeris.

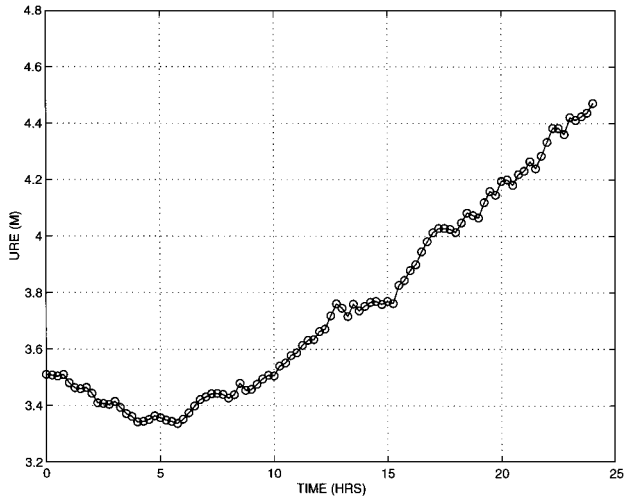

Fig. 6 URE based on EOP errors only for day 37, case 1.

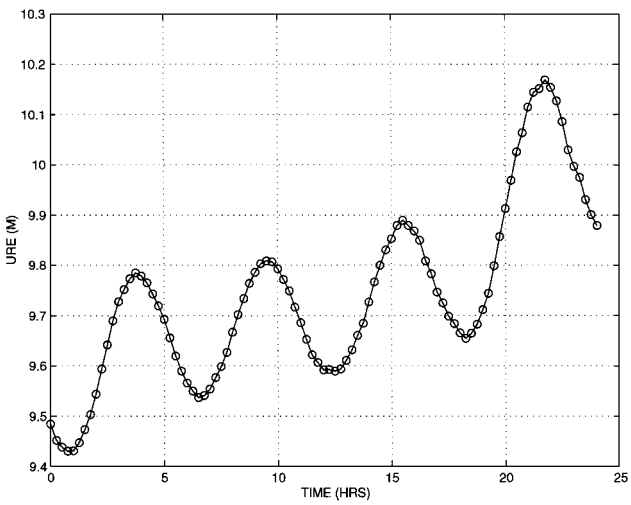

Fig. 7 URE based on EOP errors only for day 97, case 2.

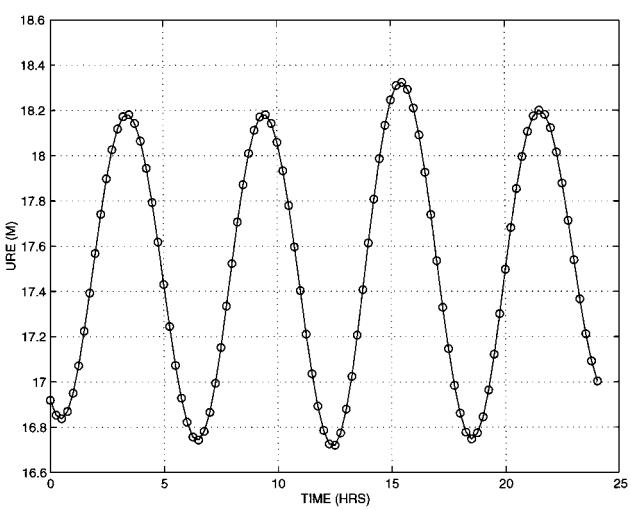

Fig. 8 URE based on EOP errors only for day 187, case 3.

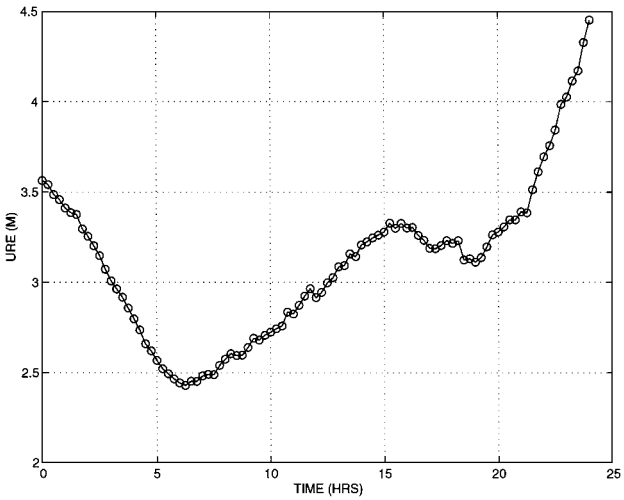

Fig. 9 URE based on ground-data-only solution for day 187, case 3.

Note that this analysis has not taken into account several other error sources such as medium effects, relativity, and noise. Note also that the URE values are based on one realization of the EOP errors and naturally would be different for other realizations. Furthermore, the UT1 error used in this analysis is pessimistic in the sense that it is about 2.6 times the rms value of UT1 error predicted for 180 days given in Table 1 of Ref. 19. The fact that performance will degrade in the autonomous mode, without ground contact, because of errors in the prediction of the orientation of the Earth is well known in the GPS autonomous navigation community.

Finally, to demonstrate the fact that the large errors (biases) in the filter estimates when cross-link measurements were processed were caused only by orbit node unobservability, range measurements from five ground stations to the GPS satellites were processed. These measurements were simulated for day 187 and processed using the same parameter estimates as in case 3. The rms of fit for the 2692 range measurements was 0.833 m, and the difference between the solution trajectory and the true trajectory was about 4 to 8 m rms (as opposed to the 1500-m level shown in Table 6). Figure 9 shows the URE computed on the basis of this error of the orbit/clock solution. It is clear that the URE mean is about 3.1 m and stays well below 5 m for entire day, illustrating that the UT1 error does not dominate when ground measurements are processed and further that there is no unobservability problem causing large bias in the filter solution.

Summary and Conclusion

Some of the autonomous navigation aspects of the GPS Block IIR satellites using stored navigation messages and cross-link pseudorange measurements were studied using a numerical simulation. Realistic force and measurement models were used in the analysis, accounting for major error sources. Real EOPs were used in the simulation. Prediction intervals of 30, 90, and 180 days were considered. Cross-link measurements for a period of one day were generated at the end of each of these prediction intervals and were processed in a least-squares estimation scheme. The estimated solutions then were compared with the true solutions to evaluate the effect of prediction errors.

The cross-link solutions indicate that the prediction error caused by force-model and clock-model errors can be corrected by using cross-link measurements. However, because of the nature of these measurements, the solution is ambiguous in the estimate of the orbit plane's ascending node and results in large differences when compared with the true values, thereby obscuring the effect of EOP errors. Note that these large differences given in Table 5 do not really represent system performance and are not very relevent to the main results of the paper. Consequently, the effect of EOP errors are determined essentially by direct differencing of trajectories computed in the true and the predicted reference frames. The UREs computed from these trajectory and clock differences for the case of 90-day prediction exceed 9 m and those corresponding to the case of 180-day prediction exceed 17 m.

In conclusion, note that the 180-day predicted ephemeris stored onboard the satellite contains errors originating from two separate sources, namely the force-model errors and the EOP errors. The part of the ephemeris error caused by force model (and initial conditions) can be corrected by the onboard filter using the cross-link measurements, whereas the part caused by EOP prediction error cannot be corrected using cross-link measurements. Hence, the additional measures mentioned earlier necessitate that either 1) a substantially improved technique for predicting UT1 must be developed or 2) a tie from the GPS constellation to the Earth's surface must be incorporated by a surface-based tracking system.

References

[1]Parkinson, B. W., Stansell, T., Beard, R., and Gromov, K., "A History of Satellite Navigation," *Journal of the Institute of Navigation*, Vol. 42, No. 1, 1995, pp. 109–164.

[2]Bowen, R., Swanson, P. L., Winn, F. B., Rhodus, N. W., and Feess, W. A., "Global Positioning System Operational Control System Accuracies," *Global Positioning System*, edited by S. W. Gilbert, Vol. 3, Navigation Series, Inst. of Navigation, Alexandria, VA, 1986, pp. 241–257.

[3]Van Dierendock, A. J., Russell, S. S., Kopitzke, E. R., and Birnbaum, M., "The GPS Navigation Message," *Journal of the Institute of Navigation*, Vol. 25, No. 2, 1978, pp. 55-73.

[4]"Interface Control Document," Satellite Systems Div., Rockwell International Corp., ICD-GPS-200, rev. B, Downey, CA, Nov. 1987.

[5]Ananda, M. P., Berstein, H., Bruce, R. W., Cunningham, K. E., Feess, W. A., Jorgensen, P. S., Menn, M., and Price, C. M., "Autonomous Navigation of the Global Positioning System Satellites," AIAA Paper 84-186, Aug. 1984.

[6]Codik, A., "Autonomous Navigation of GPS Satellites: A Challenge for the Future," *Proceedings of National ION Technical Meeting* (San Diego, CA), Inst. of Navigation, Alexandria, VA, 1985.

[7]Menn, M., "Autonomous Navigation for GPS via Cross-Link Ranging," Inst. of Electrical and Electronics Engineers Position Location and Navigation Symposium, Inst. of Electrical and Electronics Engineers, New York, 1986, pp. 143–146.

[8]Ananda, M. P., Bernstein, H., Cunningham, K. E., Feess, W. A., and Stroud, E. G., "Global Positioning System (GPS) Autonomous Navigation," Inst. of Electrical and Electronics Engineers Position Location and Navigation Symposium, Inst. of Electrical and Electronics Engineers, New York, 1990, pp. 497–508.

[9]Tapley, B. D., Watkins, M. M., Ries, J. C., Davis, G. W., Eanes, R. J., Poole, S. R., Rim, H. J., Schutz, B. E., Shum, C. K., Nerem, R. S., Lerch, F. J., Marshall, J. A., Klosko, S. M., Pavis, N. K., and Williamson, R. G., "The Joint Gravity Model 3," *Journal of Geophysical Research*, Vol. 101, No. B12, 1996, pp. 28,029–28,049.

[10]Fliegel, H. F., Gallini, T. E., and Swift, E. R., "Global Positioning System Radiation Force Model for Geodetic Applications," *Journal of Geophysical Research*, Vol. 97, No. B1, 1992, pp. 559–568.

[11]Hellwig, H., "Microwave Time and Frequency Standards," *Radio Science*, Vol. 14, No. 4, 1979, pp 561–572.

[12]Fell, P. J., and Hermann, B. R., "An Empirical Evaluation of the Effect of Oscillator Errors on Dynamic Point Positioning Based on the NAVSTAR GPS System," *Proceedings of the Second International Geodetic Symposium on Satellite Doppler Positioning* (Austin, TX), Applied Research Labs., Univ. of Texas, Austin, TX, 1979, pp 1193–1234.

[13]Meditch, J. S., "Clock Error Models for Simulation and Estimation," The Aerospace Corp., Rept. TOR-0076 (6474-D1)-2, El Segundo, CA, July 1975.

[14]"Department of Defense World Geodetic System 1984: Its Definition and Relationships with Local Geodetic Systems," Defense Mapping Agency, DMA TR-8350.2, Washington, DC, 1987.

[15]Soler, T., and Hothem, L. D., "Coordinate Systems Used in Geodesy: Basic Definitions and Concepts," *Journal of Surveying Engineering*, Vol. 114, No. 2, 1988, pp. 84–97.

[16]Menn, M. D., and Bernstein, H., "Ephemeris Observability Issues in the Global Positioning System (GPS) Autonomous Navigation (AUTONAV)," Inst. of Electrical and Electronics Engineers Position Location and Navigation Symposium, Inst. of Electrical and Electronics Engineers, New York, 1994.

[17]Bernstein, H., Bowen, A. F., and Gartside, J. H., "GPS User Position Accuracy with Block IIR Autonomous Navigation," *Proceedings of the ION GPS-93* (Salt Lake City, UT), Inst. of Navigation, Alexandria, VA, 1993, pp. 1389–1399.

[18]Bernstein, H., "Calculation of User Range Error (URE) Variances from a Global Positioning Satellite (GPS)," The Aerospace Corp., Rept. TOR-0083 (3476-02)-1, El Segundo, CA, June 1983.

[19]Kosek, W., McCarthy, D. D., and Luzum, B., "Possible Improvement of Earth Orientation Forecast Using Autocovariance Prediction Procedures," *Journal of Geodesy* (to be published).